Journal of Applied Mathematics and Physics, 2023, 11, 618-628
https://www.scirp.org/journal/jamp
ISSN Online: 2327-4379
ISSN Print: 2327-4352

Effects of Adaptive Random Deceleration on Traffic Flow

Qi Wang[1], Shu Zhu[2], Liuhua Zhu[2,3,4*]

[1]School of computer, Jiangsu University of Science and Technology, Zhenjiang, China
[2]School of Physics and Telecommunication Engineering, Yulin Normal University, Yulin, China
[3]Guangxi Colleges and Universities Key Laboratory of Complex System Optimization and Big Data Processing, Yulin, China
[4]Optoelectronic Information Research Center, Yulin Normal University, Yulin, China
Email: *lhzhu@ylu.edu.cn

How to cite this paper: Wang, Q., Zhu, S. and Zhu, L.H. (2023) Effects of Adaptive Random Deceleration on Traffic Flow. *Journal of Applied Mathematics and Physics*, **11**, 618-628.
https://doi.org/10.4236/jamp.2023.113039

Received: February 7, 2023
Accepted: March 6, 2023
Published: March 9, 2023

Abstract

Based on the Nagel-Schreckenberg model, an improved cellular automaton traffic flow model is proposed, in which the random deceleration probability of each vehicle is no longer fixed, but is adaptively adjusted according to the local traffic density in its vision and its current velocity. The numerical simulation results show that the maximum traffic capacity of the improved model under the same parameters is greater than that of the Nagel-Schreckenberg model, and is closer to the measured data. In addition, the traffic flow and vehicle velocity under different meteorological conditions are simulated by using the improved model, and the synchronized flow phenomenon consistent with the actual traffic is reproduced. Meanwhile, the results show that under the same parameters, when the traffic density is equal to 0.3, the traffic flow of the improved model increases by about 11% compared with the original model, and when the traffic density increases to 0.6, the traffic flow increases by about 27%.

Keywords

Traffic Flow, Cellular Automaton, Adaptive Random Deceleration, Synchronized Flow

1. Introduction

In recent years, the problem of traffic flow has attracted widespread attention of the scientific community due to its complex nonlinearity and the non-equilibrium phase transition observed in the actual measurement, and has gradually become an important subject of current scientific research. There are three kinds of models commonly used in traffic flow research: hydrodynamics model based on

continuous description, gas-kinetics model based on probabilistic description, and cellular automaton model based on discrete description [1] [2] [3] [4] [5].

The traffic flow composed of a large number of vehicles is actually a discrete system, so it has unique advantages to use the essentially discrete cellular automaton model to describe the actual traffic phenomenon. The cellular automaton traffic flow models can flexibly set vehicle operation rules according to the actual situation, and have good parallelism, so they have been widely used in the field of traffic flow research. Among them, the most famous model is the one-dimensional cellular automaton traffic flow model, referred to as NaSch model [6], proposed by two German scholars Nagel and Schreckenberg in 1992.

The NaSch model divides the lane into a one-dimensional lattice chain with equal distance, and labels all vehicles from left to right, which are $1,2,3,\cdots,N$, where the position of the ith vehicle is marked as x_i, and its velocity is marked as v_i, and assumes that all vehicles have the same maximum velocity $v_{\max}$. The vehicle motion is updated in parallel according to the following rules. (R1) Deterministic acceleration, $v_i\left(t+1/3\right)=\min\left\{v_i\left(t\right)+1,v_{\max}\right\}$; (R2) Deterministic deceleration, $v_i\left(t+2/3\right)=\min\left\{d_i\left(t\right),v_i\left(t+1/3\right)\right\}$, in which $d_i\left(t\right)=x_{i+1}\left(t\right)-x_i\left(t\right)-1$; (R3) Random deceleration, $v_i\left(t+1\right)=\max\left\{v_i\left(t+2/3\right)-1,0\right\}$. This behavior occurs with probability p; (R4) Updating of position, $x_i\left(t+1\right)=x_i\left(t\right)+v_i\left(t+1\right)$. This classic model takes into account the stochastic slowing of uncertainty, and shows the phase transition of vehicle flow from free moving phase to local blocking phase for the first time, which has attracted wide attention from the international academic community.

2. Model

Although the developed transportation has brought endless convenience to people, it has also increased many security risks. Vehicle overspeed, overload, overrun and other behaviors violating the road traffic safety law will lead to frequent traffic accidents. At present, the vast majority of traffic safety accidents occur in severe weather conditions (rain, snow, ice on the road, fog, etc.), so it is particularly important for every driver to drive safely under the adverse conditions. The impact of adverse weather conditions on driver's driving behavior mainly includes the following three aspects: the first is braking distance and braking characteristics; the second is the driver's vision; the third is the behaviors of other traffic participants on the road [7] [8] [9].

The real traffic scenario is as follows: when the traffic density in the driver's field of vision is large, the vehicle spacing is small, and the deceleration probability is large, otherwise, the reverse. The higher the vehicle velocity, the greater the probability of accidents between vehicles. Once a vehicle decelerates suddenly, it will cause the following vehicles to have no time to decelerate and cause accidents. Therefore, the higher the vehicle velocity, the greater the deceleration probability.

So we have reason to believe that there is a certain correlation between the random deceleration probability and the traffic density in the driver's field of vi-

sion and the velocity of the target vehicle [10] [11] [12] [13] [14]. We assume that the correlation function is $p = \rho_l^{\alpha}\left[v/v_{\max}\right]^{\beta}$, in which ρ_l is the local traffic density within the driver's field of vision, l is the driver's visual distance, α and β are adjustable power exponents for different road conditions and weather conditions. The value of ρ_l is calculated by the formula $\rho_l(x) = \frac{1}{l}\sum_{n=x+1}^{x+l}\lambda_n$. Here x is the position of the target vehicle, λ_n is a Boolean variable. If the nth lattice is occupied by a vehicle, then $\lambda_n = 1$, otherwise $\lambda_n = 0$.

We only make one improvement on the NaSch model, that is, replace the constant random deceleration probability with the adaptive random deceleration probability. Consequently, we need to determine the adaptive random deceleration probability before the evolution rules of the original NaSch. Thus, (R0) $p_i(t) = \left[\rho_l\left(x_i(t)\right)\right]^{\alpha}\left[v_i(t)/v_{\max}\right]^{\beta}$ is added to the original NaSch model, in which i is the identifier of the vehicle, $x_i(t)$ and $v_i(t)$ are its position and velocity at time t respectively. The rule R0 here and the rules from R1 to R4 in the introduction constitute the whole of the improved model.

In this simulation, we use a one-dimensional discrete lattice chain with length $L = 1000$ to represent a one-way lane. In order to ensure the constant number of vehicles on the road, the periodic boundary condition is adopted. Each cell corresponds to a road with an actual length of 6 m. Unless otherwise stated, the maximum velocity of the vehicle is set to $v_{\max} = 5$, which is equivalent to the actual velocity of 108 km/h.

3. Results

In this section, we report the impact of adaptive random deceleration on road traffic. The common method is to introduce two parameters, namely average velocity and traffic flow. The average velocity is given by the calculation formula $\bar{v} = \frac{1}{N}\sum_{i=1}^{N} v_i$, in which N is the total number of vehicles on the road. The traffic flow is obtained from the calculation formula $J = \rho\bar{v}$, in which $\rho = N/L$ is the global traffic density. We change the deceleration probability values in the simulation process by adjusting the values of α and β, thus affecting the change trend of corresponding traffic flow and average velocity.

Figure 1(a) shows the relationship between average velocity and traffic flow of the improved model. Each data point in **Figure 1(b)** is obtained by averaging the measured data within 6 minutes on a highway in California [15]. Comparing **Figure 1(a)** with **Figure 1(b)**, we can find that the maximum traffic flow obtained by numerical simulation is very close to the measured data. Obviously, the improved model proposed in this paper can truly reflect the nonlinear relationship between velocity and flow in actual traffic. In the initial free flow phase, the traffic density is small, and all vehicles can freely choose the desired driving velocity, so the average velocity of the system is roughly equal to the maximum allowable velocity. When the traffic density is higher than the critical point, with the

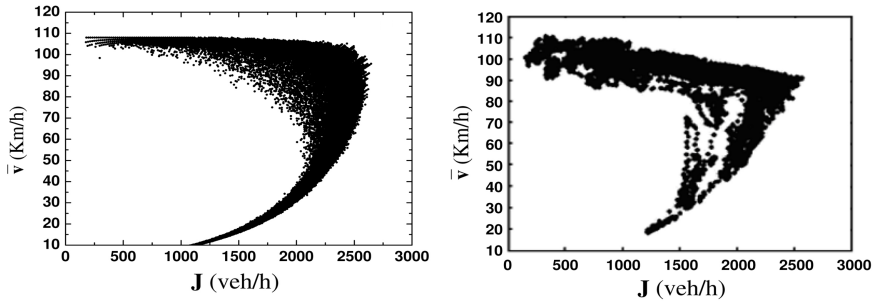

Figure 1. The relationship diagrams between average velocity and traffic flow obtained from two kinds of different ways. (a) the numerical simulation; (b) the actual measurement. The parameters are set to $v_{\max}=5$, $l=30$, $\alpha=1.0$ and $\beta=1.0$ in the left panel.

increase of traffic density, the traffic flow gradually changes from free flow to the wide moving jam, and some areas begin to appear blocking, resulting in a rapid decline in traffic flow. In the velocity-flow diagram, the curve quickly regresses from the maximum flow point to the origin where the velocity and flow are both zero.

In order to visualize the evolution process of vehicles from free movement phase to blocking phase, we simulate the relationship diagram between vehicle position and movement time during vehicle movement. The simulated spatial position range is 200 - 700, and the time step is 10,200 - 10,600. The parameters are set to $v_{\max}=5$, $l=30$, $\alpha=1.0$ and $\beta=1.0$.

Figure 2(a) shows the relationship between vehicle position and movement time at $\rho=0.15$, where a black dot represents a vehicle. The density of vehicles on the lane is low, and the traffic flow is in a free flow state. With the increase of time, the vehicle moves forward, and the position changes almost linearly with time. In order to clearly see the change of vehicle velocity, we draw the evolution diagram of vehicle velocity with time, as shown in **Figure 2(b)**. **Figure 2(b)** shows that most vehicles can drive at maximum velocity, but with the passage of time, there will be sporadic low-velocity vehicles on the road. The distribution of vehicles is relatively uniform, and there is no static vehicle on the road.

Each data point in **Figure 3(a)** is obtained by averaging the respective random deceleration probability of each vehicle within 1000 time steps. The statistical average value of adaptive random deceleration probability of all vehicles on the current lane is equal to 0.127. **Figure 3(b)** shows the space-time evolution of the classic NaSch model with the same parameters. The only difference between the current model and the classic NaSch model is that the random deceleration probability of the current model is uneven, and their average value is 0.127. In the NaSch model, each vehicle has the same random deceleration probability, and they all take 0.127. It can be seen from **Figure 3(b)** that there are some sporadic static vehicles on the lane and form some small blocking areas, but they soon dissipate and the whole lane is in a state of oversaturation. Comparing **Figure 2(a)** with **Figure 3(b)**, we find that the improved model obtains a more

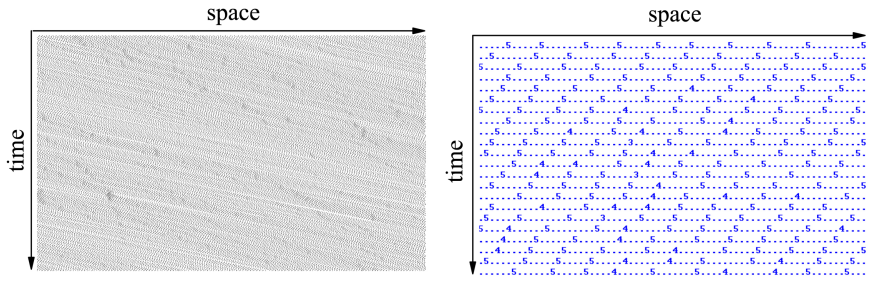

Figure 2. The spatial-temporal diagram (left panel) and the snapshot of velocity evolution (right panel) of the present model at the traffic density $\rho = 0.15$. The right panel depicts the details of the left panel. Due to the space limitation, the right panel only describes a small amount of information on the left panel, not all of it. The vehicles are moving from left to right. A vehicle is represented by a black dot in the left panel. The vehicle is represented by its velocity value in the right panel, while an empty cell is depicted with a blue dot. The time axis is vertical down. Other parameters are set to $v_{\max} = 5$, $l = 30$, $\alpha = 1.0$ and $\beta = 1.0$.

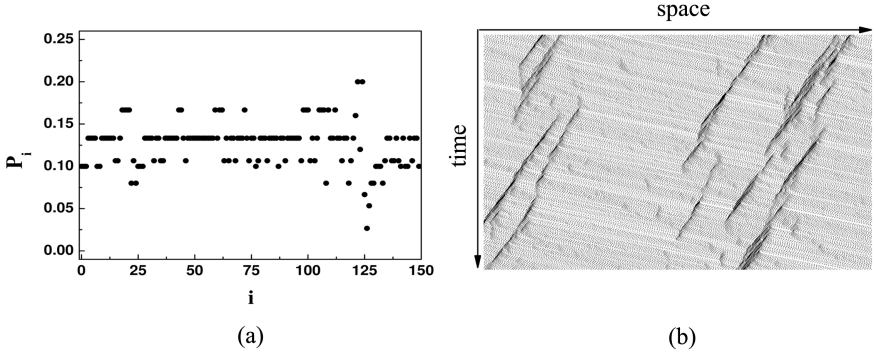

Figure 3. (a) The statistical average diagram of adaptive random deceleration probability of each vehicle in the present model. The statistical average value of adaptive random deceleration probability of all vehicles is equal to 0.127. (b) The spatial-temporal diagram of the NaSch model for $p = 0.127$ at the traffic density $\rho = 0.15$. Other parameter settings in **Figure 3(b)** are also equivalent to **Figure 2(a)**. The only difference between the present model and the NaSch model is that the random deceleration probability in this paper is adaptive, while the NaSch model treats each vehicle in a fixed way.

homogeneous space-time evolution diagram under the same parameters, which improves the traffic capacity of the road.

We change the values of α, keep $\beta = 1$ unchanged, and obtain a series of fundamental graphs, as shown in **Figure 4(a)**. By the way, the fundamental diagram in the traffic flow theory is the common name of the curve of flow changing with density. The findings suggest that the parameter α only affects traffic flow at medium density, and has little effect on the traffic flow at low and high density areas. The relationship curves between average velocity and density under the same parameters are shown in **Figure 4(b)**. The difference of the four curves in **Figure 4(b)** mainly occurs in the low density areas. At the same density, the greater the value of α, the greater its average velocity. With the increase

of density, the influence of α on the deceleration probability gradually decreases until it disappears, resulting in the final overlap of the four curves.

Next, we change the values of β, keep $\alpha = 1$ unchanged, and obtain a series of fundamental graphs, as shown in Figure 5(a). When $\beta \neq 0$, the traffic flow is not sensitive to the change of β, and the weak impact only occurs in the medium density areas. The relationship curve between flow and density at $\beta = 0$ is obviously different from that at $\beta \neq 0$. In other words, it is impractical to ignore the influence of vehicle velocity in adaptive random deceleration probability. The relationship curves between average velocity and density under the same parameters are shown in Figure 5(b). In low-density areas, the traffic flow is at the stage of unimpeded traffic, and all vehicles are expected to travel at maximum velocity. However, affected by the adaptive random deceleration probability, with the increase of density, the average velocity before the critical point decreases slightly, and the average velocity after the critical point decreases sharply. The relationship curve between average velocity and density at $\beta = 0$ is slightly different from that at $\beta \neq 0$.

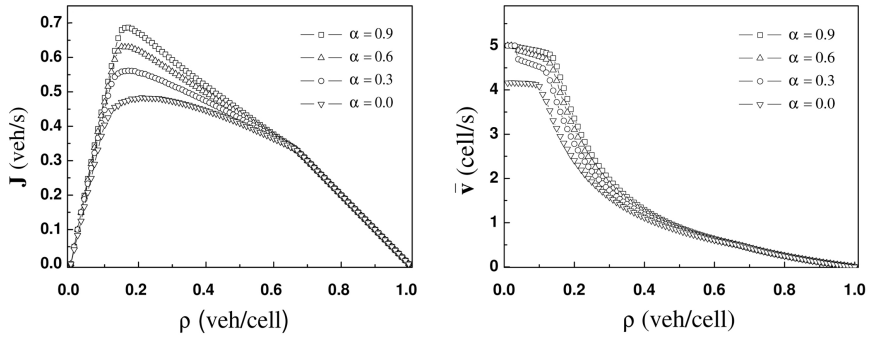

Figure 4. (a) The fundamental diagram obtained by numerical simulation. (b) The relationship diagram between average velocity and density. Besides the parameter settings on the panels, other parameters are set to $v_{\max} = 5$, $l = 30$, and $\beta = 1.0$.

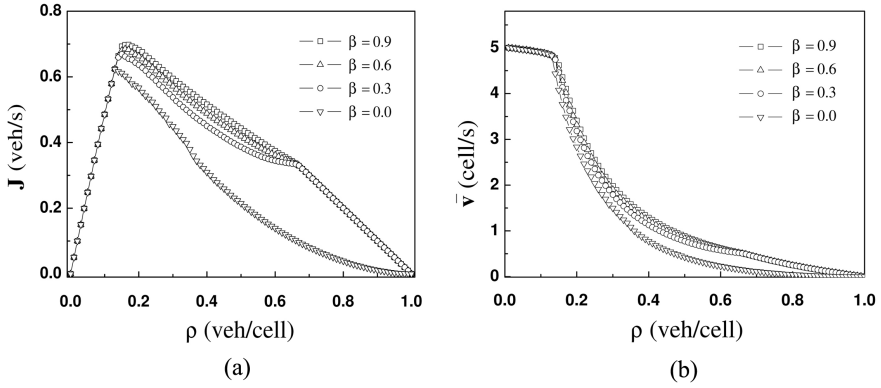

Figure 5. (a) The fundamental diagrams obtained by numerical simulation. (b) The relationship diagrams between average velocity and density. Besides the parameter settings on the panels, other parameters are set to $v_{\max} = 5$, $l = 30$, and $\alpha = 1.0$.

4. Application

The characteristics of traffic flow are different under different weather conditions. Different weather conditions, such as heavy fog, heavy precipitation, wind and snow, dust and other climatic factors, lead to reduced visibility, affecting driving velocity and traffic flow [16] [17] [18]. Our proposed model can simulate the flow, velocity and vehicle operation status under different weather conditions. Bad weather conditions can easily cause poor vision and narrow vision of drivers. In this paper, the impact of visibility on traffic flow and driving velocity is quantitatively studied. The parameter setting of the model is as follows: the maximum driving velocity will be reduced by 20% for every 30 m of visibility reduction.

The fundamental diagrams under different visibility are obtained, as shown in **Figure 6(a)**. Visibility affects the traffic capacity of roads in a large density range. Except for high-density areas, the lower the visibility, the weaker the road traffic capacity. The relationship curves between average velocity and density under the same parameters are shown in **Figure 6(b)**. In low-density areas, there are few vehicles on the road, and there is almost no vehicle in the driver's field of vision. The size of visibility does not affect the driving status, and all vehicles can drive at the expected maximum velocity. However, affected by the adaptive random deceleration probability, with the increase of density, the average velocity before the critical point decreases slightly, and the average velocity after the critical point decreases sharply.

Figure 7 shows the relationship between vehicle position and movement time at different traffic densities. At the medium traffic density, the spatiotemporal evolution diagram of the system is compact and homogeneous, as shown in **Figure 7(a)**. There is no congestion area on the lane, and all vehicles can drive at a slow velocity. The average velocity of vehicles on the whole lane is about 1.92 cell/s. However, under this density, the spatiotemporal evolution diagram of the NaSch model emerges many ghostly blockages, as shown in **Figure 8(a)**. Besides

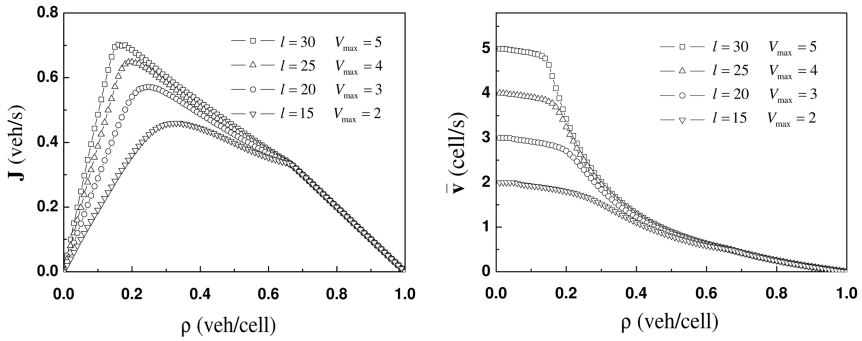

Figure 6. (a) The fundamental diagrams under different visibility obtained by numerical simulation. (b) The relationship diagrams between average velocity and density under different visibility. Besides the parameter settings on the panels, other parameters are set to $\alpha = 1.0$ and $\beta = 1.0$.

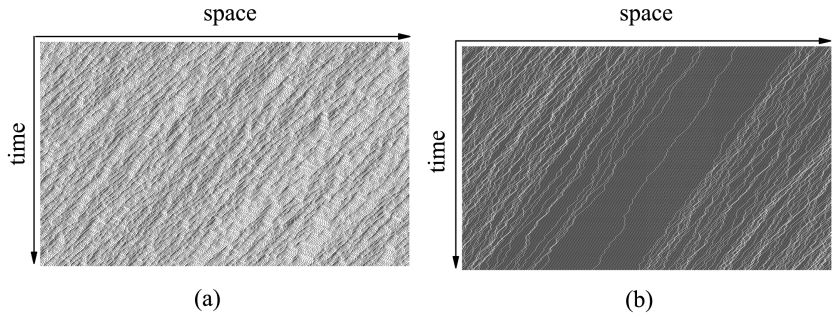

Figure 7. The spatial-temporal diagrams obtained from the current model under different traffic densities (a) $\rho = 0.3$. (b) $\rho = 0.6$. Other parameters are set to $v_{\max} = 4$, $l = 25$, $\alpha = 1.0$ and $\beta = 1.0$.

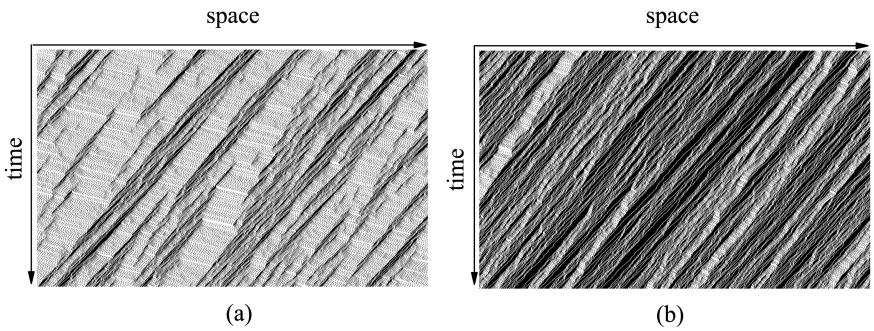

Figure 8. The spatial-temporal diagrams obtained from the NaSch model under different traffic densities (a) $\rho = 0.3$. (b) $\rho = 0.6$. The settings of other parameters are the same as those in **Figure 7**. The values of the random deceleration probability in the NaSch model are taken from the statistical averages of the adaptive random deceleration probability of all vehicles under the corresponding traffic densities in the improved model.

that, at a higher density, the system does not have a expected wide range of congestion, but has emerged a low-velocity synchronized flow consistent with the actual traffic [19] [20], as shown in **Figure 7(b)**. The average velocity of vehicles on the whole lane is about 0.62 cell/s. In **Figure 7(b)**, the area with slightly darker color and uniform texture is synchronized flow. Our proposed model makes up for the defect that NaSch model cannot reproduce a large-scale synchronized traffic flow.

The spatiotemporal evolution diagram of NaSch model is drawn when the traffic density is equal to 0.3, as shown in **Figure 8(a)**. At the medium traffic density, the driving vehicles are affected by other vehicles, and the degree of free movement is reduced. The distribution of vehicle positions is uneven, with dense vehicles in some areas and sparse vehicles in some areas. The movement of traffic flow alternates with congestion, which is very similar to the propagation of wave crest and wave trough. The average velocity of vehicles on the whole lane is about 1.73 cell/s. In addition, the evolution diagram of traffic flow is plotted when the traffic density is equal to 0.6, as shown in **Figure 8(b)**. At such a high traffic density, the local concentration of vehicles becomes larger, and there are large-scale traffic congestions in many areas. Only the vehicles in front of the

congestion areas can move, while the rest of the vehicles are waiting, resulting in a sharp decline in average velocity. The average velocity of vehicles on the whole lane is about 0.49 cell/s.

Comparing the data from **Figure 7** and **Figure 8**, we find that under the same parameters, when the traffic density is equal to 0.3, the traffic flow increases by about 11% using our proposed model, and when the traffic density increases to 0.6, the traffic flow increases by about 27%.

5. Conclusions

Based on the classic NaSch model, we consider the difference of random deceleration probability of different vehicles, and propose an improved one-dimensional cellular automaton traffic flow model. In the improved model, each vehicle is no longer assigned the same random deceleration probability in advance, but the random deceleration probability is dynamically adjusted according to the local vehicle density and the current velocity. The numerical simulation results are in good agreement with the measured data, which confirms the feasibility of the improved model.

With the help of our proposed model, the highway capacity under different visibility is simulated. The results show that when the global traffic density exceeds the critical point of the system, the traffic flow will appear a synchronous phase of slow driving rather than a large-scale congestion phase, thus improving the traffic capacity of the road, which is consistent with the actual traffic. In this paper, we only consider the periodic boundary conditions. It can be expected that under the open boundary conditions, the model is also effective, and can reproduce the nonlinear dynamic behavior in real traffic, which will be the focus of our next work.

Acknowledgements

This work is supported by the National Natural Science Foundation of China under Grant No. 61563054, and the Scientific Research Fund Project of Yulin Normal University under Grant No. G2022zk27.

Conflicts of Interest

The authors declare no conflicts of interest regarding the publication of this paper.

References

[1] Chen, Y. and Xue, G. (2022) The Adaptive Random Access Carrier Allocation Scheme in NB-IoT Networks. *Communications and Network*, **14**, 1-11. https://doi.org/10.4236/cn.2022.141001

[2] Zhu, L. (2020) Generalized Anticipation Effect Models for Traffic Flow. *Journal of Applied Mathematics and Physics*, **8**, 367-374. https://doi.org/10.4236/jamp.2020.83028

[3] Da, C., Qian, Y., Zeng, J., Zhang, Y. and Xu, D. (2022) A Cellular Automaton Model with Random Update Rules for Urban Traffic Flow. *Journal of Advanced Transportation*, **2022**, Article ID: 4607340. https://doi.org/10.1155/2022/4607340

[4] Wang, F., Li, L., Liu, Y., Tian, S. and Wei, L. (2020) One-Dimensional Cellular Automaton Traffic Flow Model Based on Defensive Driving Strategy. *International Journal of Crashworthiness*, **27**, 193-197. https://doi.org/10.1080/13588265.2020.1785091

[5] Karakhi, A., Laarej, A., Khallouk, A., Lakouari, N. and Ez-Zahraouy, H. (2021) Car Accident in Synchronized Traffic Flow: A Stochastic Cellular Automaton Model. *International Journal of Modern Physics C*, **32**, Article ID: 2150011. https://doi.org/10.1142/S012918312150011X

[6] Nagel, K. and Schreckenberg, M. (1992) A Cellular Automaton Model for Freeway Traffic. *Journal de Physique I*, **2**, 2221-2229. https://doi.org/10.1051/jp1:1992277

[7] Zhang, Y., Liu, T., Bai, Q., Shao, W. and Wang, Q. (2018) New Systems-Based Method to Conduct Analysis of Road Traffic Accidents. *Transportation Research Part F: Traffic Psychology and Behaviour*, **54**, 96-109. https://doi.org/10.1016/j.trf.2018.01.019

[8] Singh, H. and Kathuria, A. (2021) Profiling Drivers to Assess Safe and Eco-Driving Behavior—A Systematic Review of Naturalistic Driving Studies. *Accident Analysis and Prevention*, **161**, Article ID: 106349. https://doi.org/10.1016/j.aap.2021.106349

[9] Peng, Y., Chen, D., Li, X., Chen, L. and Yu, J. (2016) Research on Driving Behavior Based on Vehicles Safety. *Journal of Computational and Theoretical Nanoscience*, **13**, 2171-2180. https://doi.org/10.1166/jctn.2016.5172

[10] Orozco, S.P., Albert, S.T. and Shadmehr, R. (2021) Adaptive Control of Movement Deceleration during Saccades. *PLOS Computational Biology*, **17**, e1009176. https://doi.org/10.1371/journal.pcbi.1009176

[11] Avr, A., Tanvir, S., Rouphail, N.M. and Ahmed, I. (2021) Dynamically Collected Local Density Using Low-Cost Lidar and Its Application to Traffic Models. *Transportation Research Record: Journal of the Transportation Research Board*, **2675**, 56-67. https://doi.org/10.1177/03611981211010184

[12] Liu, C. and Zhang, W. (2022) Learning the Driver Acceleration/Deceleration Behavior under High-Speed Environments from Naturalistic Driving Data. *IEEE Intelligent Transportation Systems Magazine*, **14**, 78-91. https://doi.org/10.1109/MITS.2020.3014115

[13] Vranken, T., Sliwa, B., Wietfeld, C. and Schreckenberg, M. (2021) Adapting a Cellular Automata Model to Describe Heterogeneous Traffic with Human-Driven, Automated, and Communicating Automated Vehicles. *Physica A: Statistical Mechanics and Its Applications*, **570**, Article ID: 125792. https://doi.org/10.1016/j.physa.2021.125792

[14] Varotto, S.F., Jansen, R., Bijleveld, F. and Nes, N.V. (2021) Adaptations in Driver Deceleration Behaviour with Automatic Incident Detection: A Naturalistic Driving Study. *Transportation Research Part F: Traffic Psychology and Behaviour*, **78**, 164-179. https://doi.org/10.1016/j.trf.2021.02.011

[15] Xue, Y., Dong, L. and Dai, S. (2001) An Improved One-Dimensional Cellular Automaton Model of Traffic Flow and the Effect of Deceleration Probability. *Acta Physica Sinica*, **50**, 445-449. https://doi.org/10.7498/aps.50.445

[16] Mathew, S. and Pulugurtha, S.S. (2022) Quantifying the Effect of Rainfall and Visibility Conditions on Road Traffic Travel Time Reliability. *Weather, Climate, and*

Society, **14**, 507-519. https://doi.org/10.1175/WCAS-D-21-0053.1

[17] Zhang, X. and Gao, J. (2019) Research on the Fixation Transition Behavior of Drivers on Expressway in Foggy Environment. *Safety Science*, **119**, 70-75. https://doi.org/10.1016/j.ssci.2018.08.020

[18] Sun, S., Hu, J. and Wang, R. (2021) Correlation between Visibility and Traffic Safety Visual Distance in Foggy Areas during the Daytime. *Traffic Injury Prevention*, **22**, 514-518. https://doi.org/10.1080/15389588.2021.1916924

[19] Tian, J., Zhu, C., Jiang, R. and Treiber, M. (2021) Review of the Cellular Automata Models for Reproducing Synchronized Traffic Flow. *Transportmetrica A*: *Transport Science*, **17**, 766-800. https://doi.org/10.1080/23249935.2020.1810820

[20] Li, Q., Fu, D., Jiang, R. and Wang, B. (2022) A Refined Cellular Automaton Model with Dual Cruise-Control Limit for Reproducing Synchronized Traffic Flow. *International Journal of Modern Physics C*, **33**, Article ID: 2250114. https://doi.org/10.1142/S0129183122501145